Electronic Supplementary Information

Electrochemical oxygen evolution catalysis of metal sulfides: a systematic study of electronic effects

Yuuki Sugawara,[a] Taisei Uchiyama,[a] Maxim Shishkin[‡a] and Takeo Yamaguchi*[a]

[a]*Laboratory for Chemistry and Life Science, Institute of Integrated Research, Institute of Science Tokyo, R1-17, 4259 Nagatsuta-cho, Midori-ku, Yokohama, Kanagawa 226-8501, Japan*

[‡]*(present address) Department of Transdisciplinary Science and Engineering, School of Environment and Society, Institute of Science Tokyo, 2-12-1 Ookayama, Meguro-ku, Tokyo, 152-8552, Japan*

*Corresponding author E-mail: yamag@res.titech.ac.jp.

Supplementary Figures and Tables

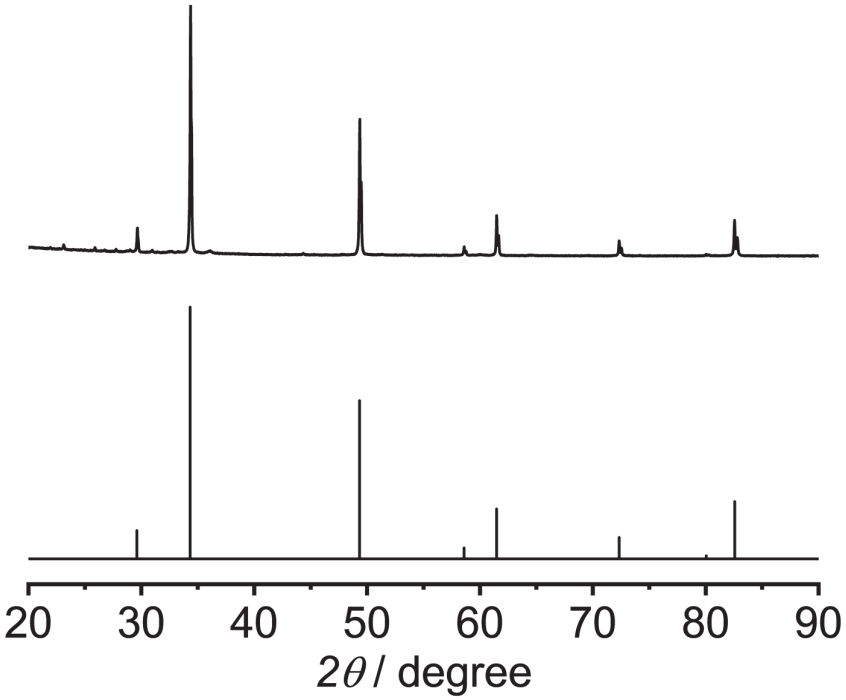

Fig. S1 Measured (upper) and theoretical (lower; JCPDS: 03-065-2919) X-ray diffraction (XRD) patterns of MnS.

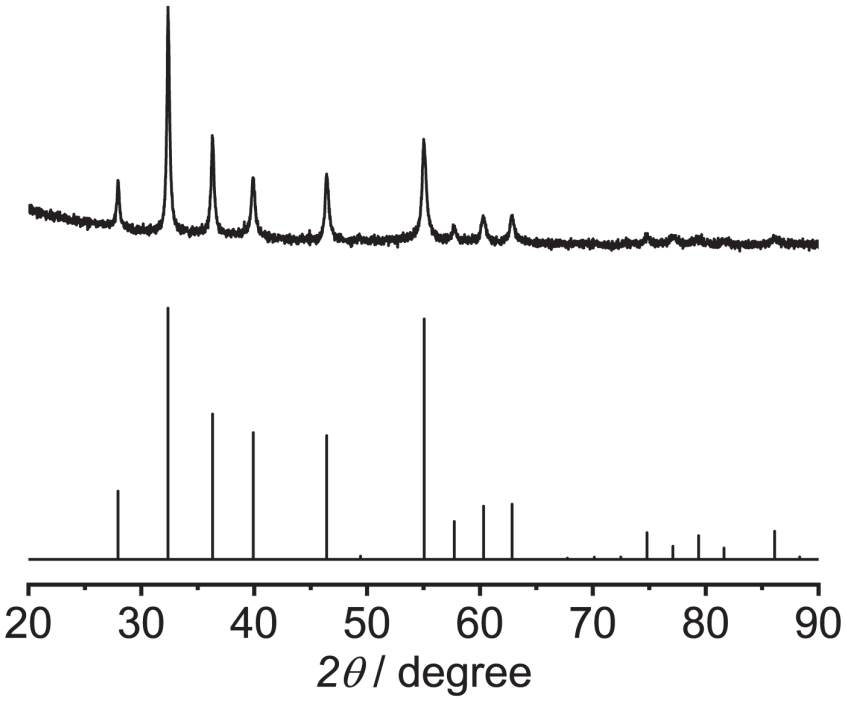

Fig. S2 Measured (upper) and theoretical (lower; JCPDS: 04-003-1962) XRD patterns of CoS_2.

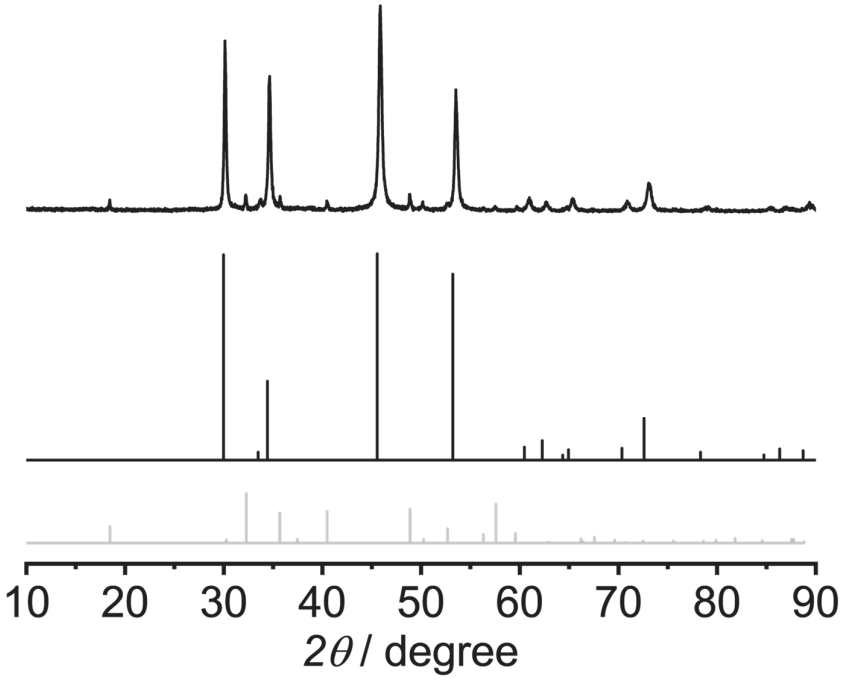

Fig. S3 Measured (upper) and theoretical (middle; JCPDS: 01-089-1957) XRD patterns of α-NiS. The sample contains 3.1% of β-NiS (lower; ICSD: 29312).

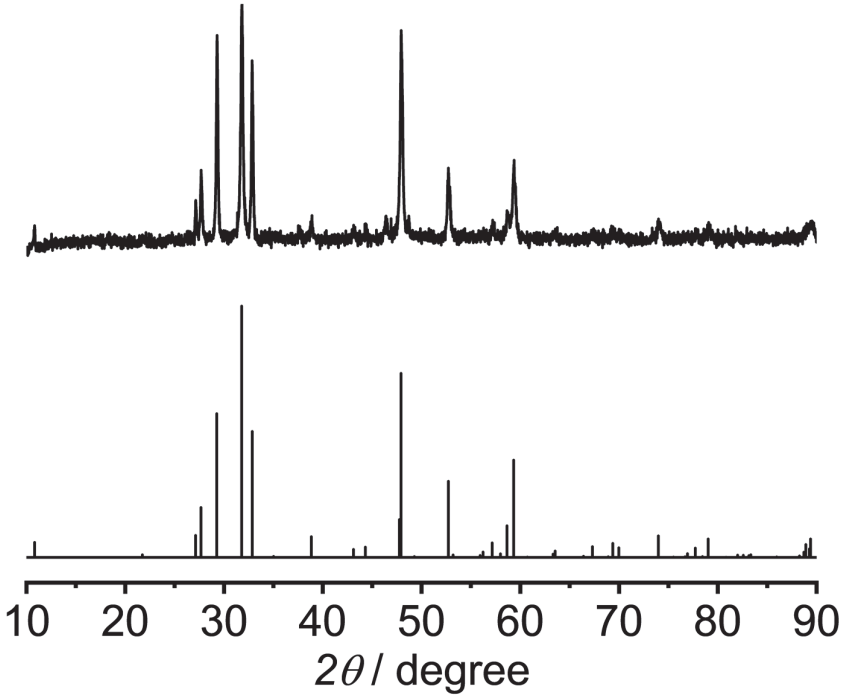

Fig. S4 Measured (upper) and theoretical (lower; JCPDS: 04-008-8460) XRD patterns of CuS.

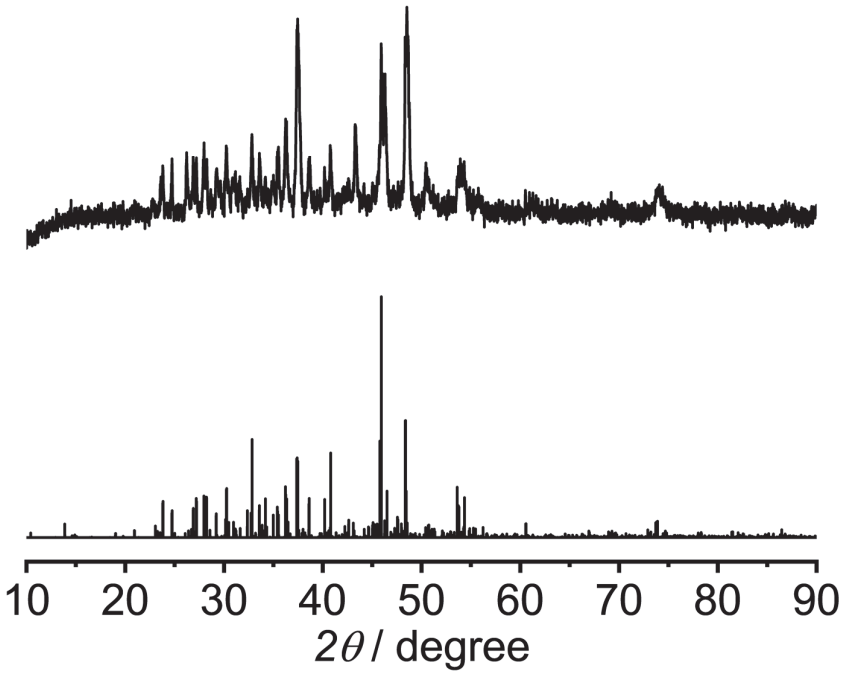

Fig. S5 Measured (upper) and theoretical (lower; JCPDS: 04-024-2239) XRD patterns of Cu_2S.

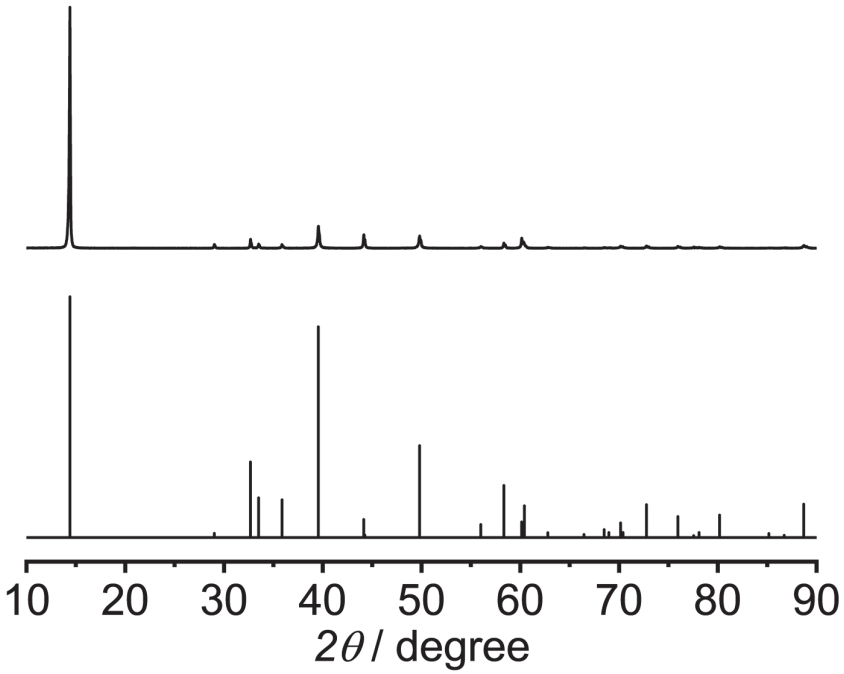

Fig. S6 Measured (upper) and theoretical (lower; JCPDS: 00-037-1492) XRD patterns of MoS_2.

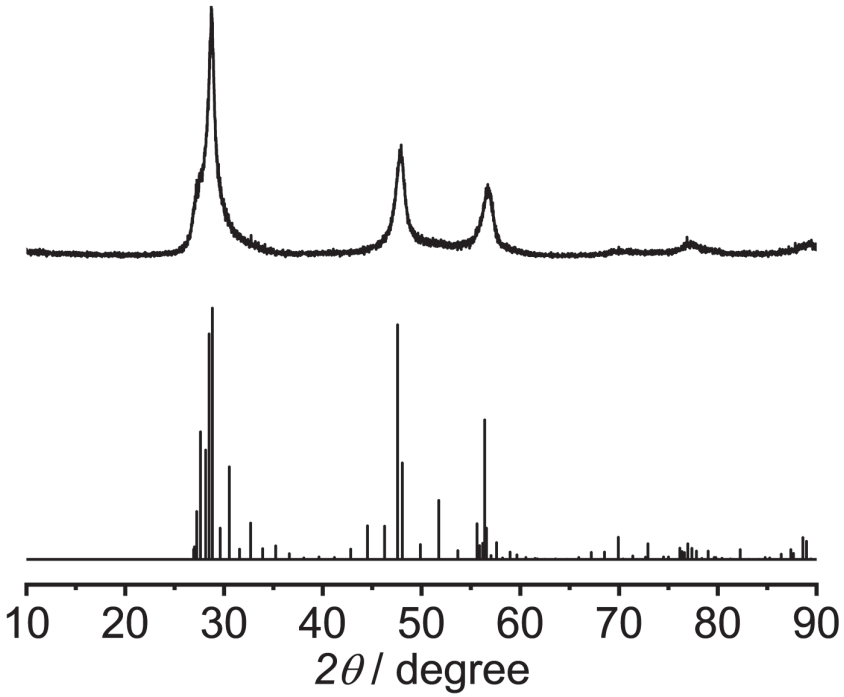

Fig. S7 Measured (upper) and theoretical (lower; JCPDS: 01-074-5022) XRD patterns of ZnS.

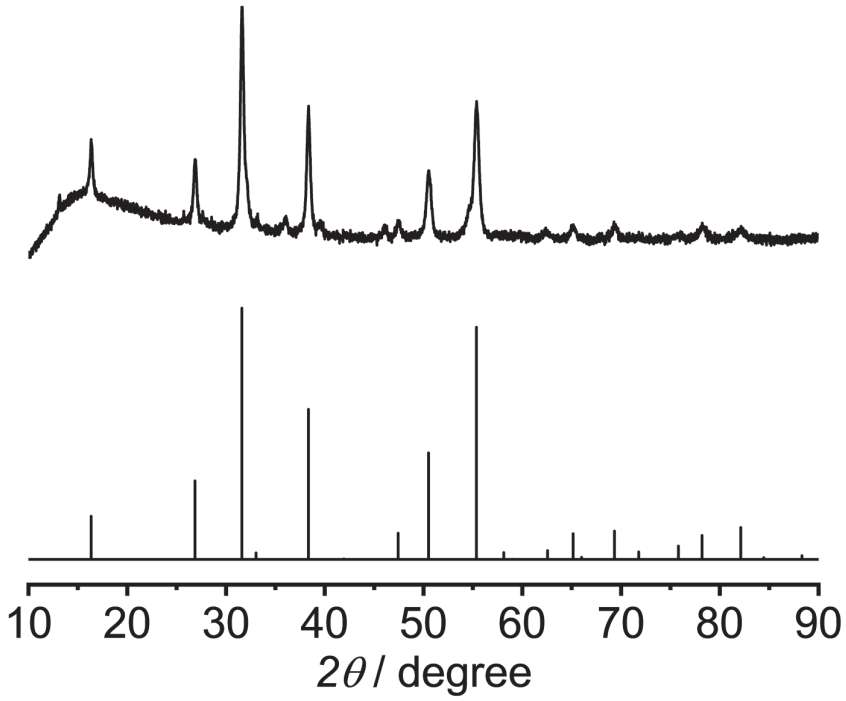

Fig. S8 Measured (upper) and theoretical (lower; JCPDS: 01-073-1704) XRD patterns of $NiCo_2S_4$.

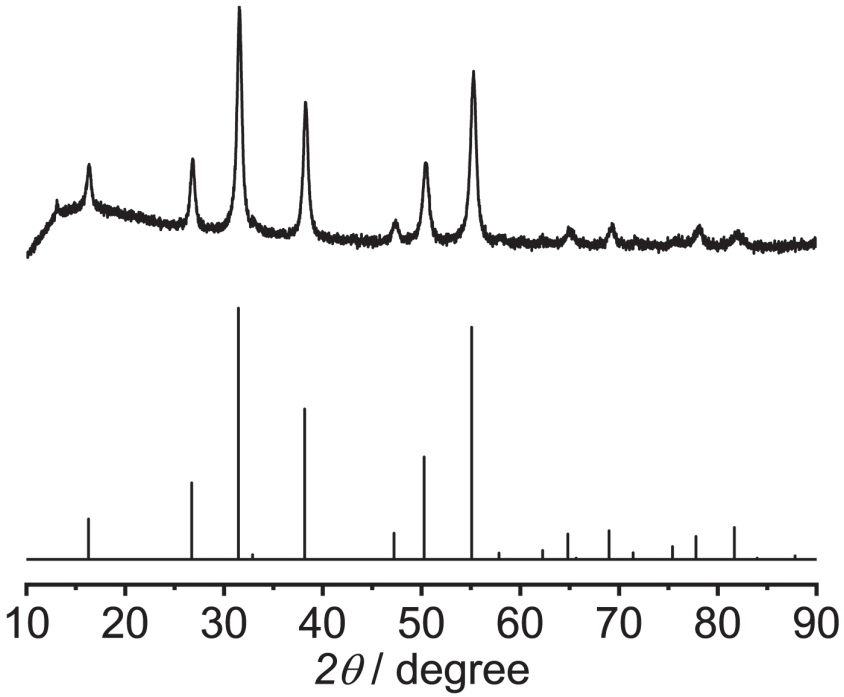

Fig. S9 Measured (upper) and theoretical (lower; JCPDS: 01-073-1297) XRD patterns of $CoNi_2S_4$.

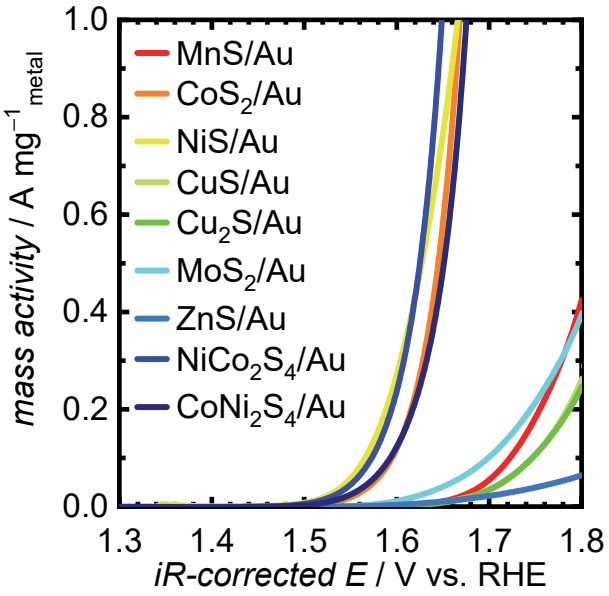

Fig. S10 OER polarization curves of the metal sulfides in 1 M KOH based on the mass activity.

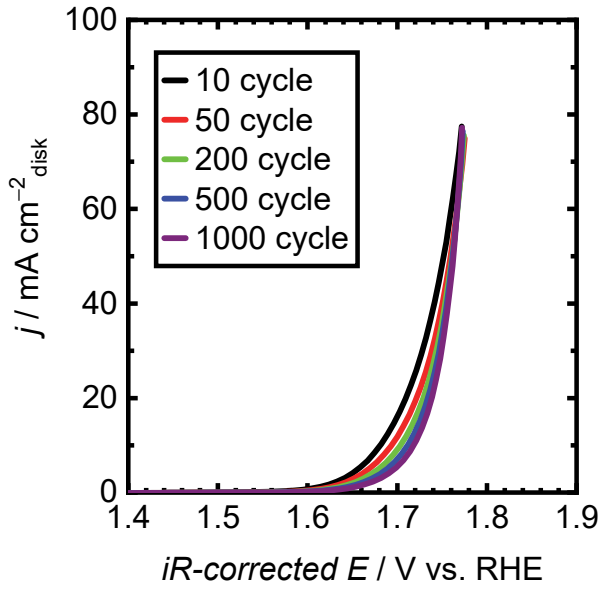

Fig. S11 OER polarization curves of CoS_2/Au electrode after repeated potential cycles.

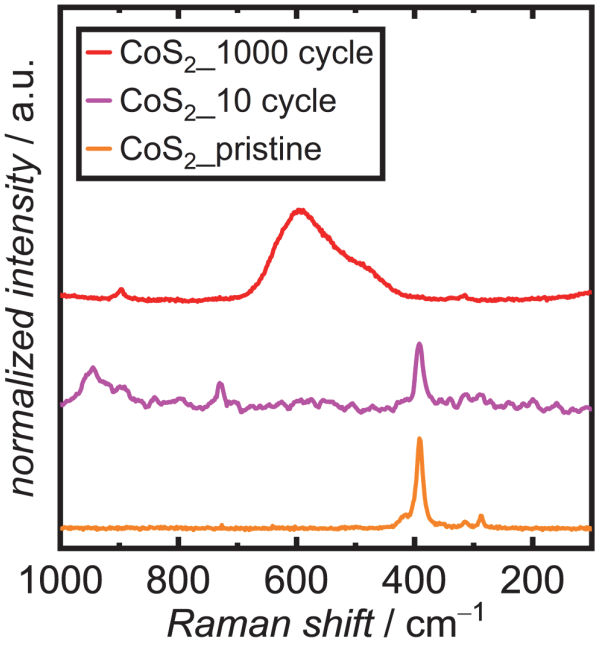

Fig. S12 Raman spectra of pristine CoS_2 and recovered samples from CoS_2/Au electrode after 10 and 1000 cycles.

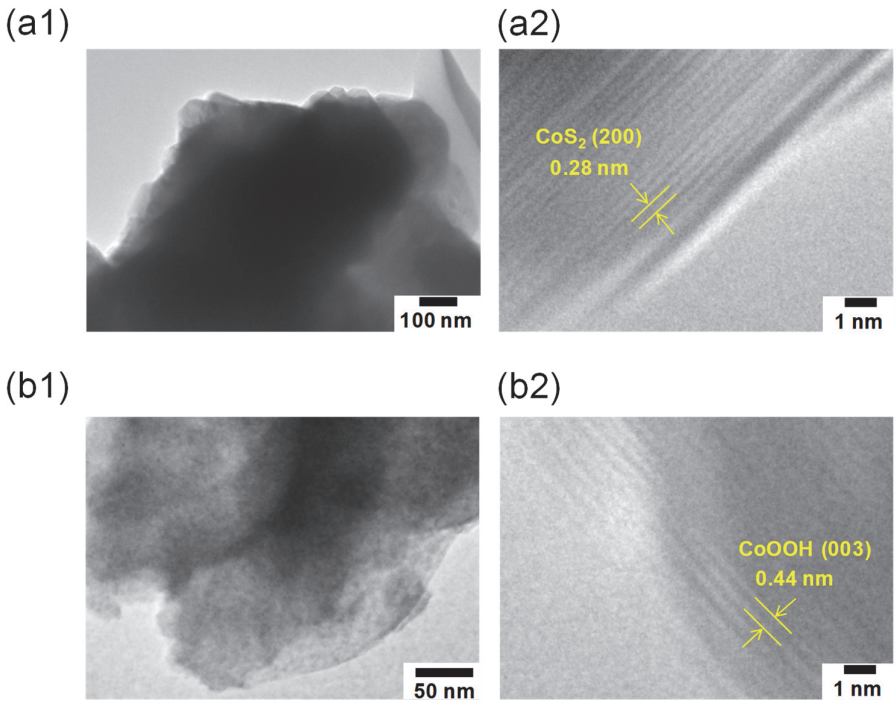

Fig. S13 TEM images of the (a1) pristine CoS_2, (b1) its recovered sample after 1000 repeated potential cycles and their zoomed images (a2 and b2).

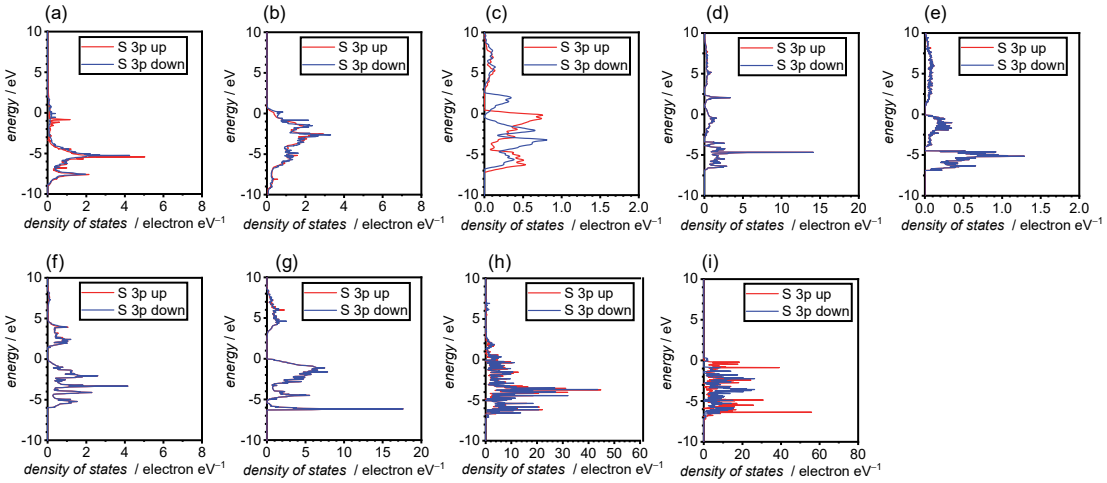

Fig. S14 DFT-calculated PDOS of the sulfur *p* band for the metal sulfides. (a) MnS, (b) CoS_2, (c) NiS, (d) CuS, (e) Cu_2S, (f) MoS_2, (g) ZnS, (h) $NiCo_2S_4$ and (i) $CoNi_2S_4$.

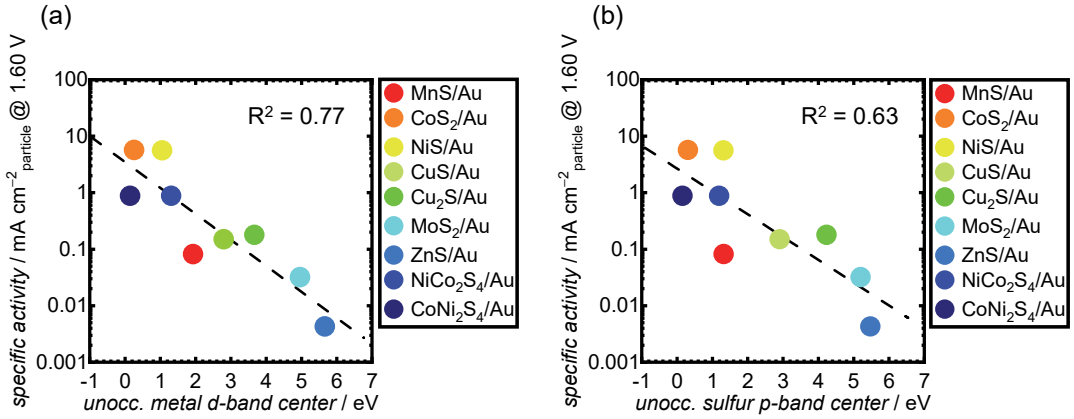

Fig. S15 OER specific activity at 1.60 V for the metal sulfides as a function of the unoccupied (a) metal *d*- and (b) sulfur *p*-band centers for each metal sulfide, extracted from the DFT-obtained PDOS presented in Fig. 6 and S14, respectively.

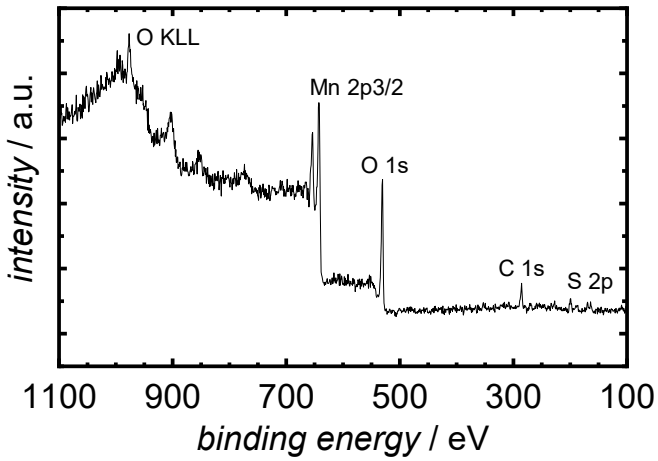

Fig. S16 XPS spectrum of MnS.

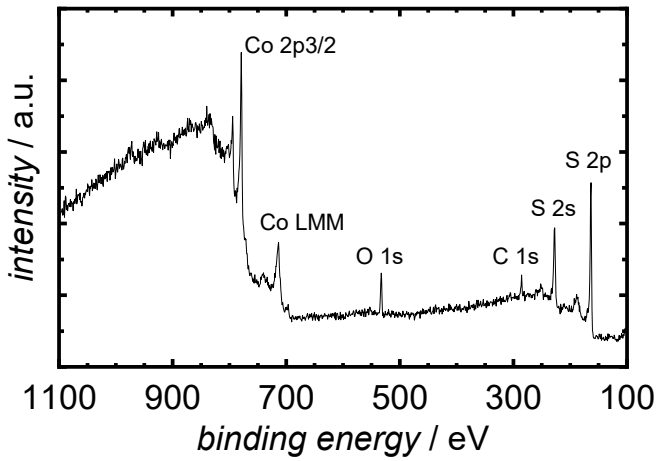

Fig. S17 XPS spectrum of CoS_2.

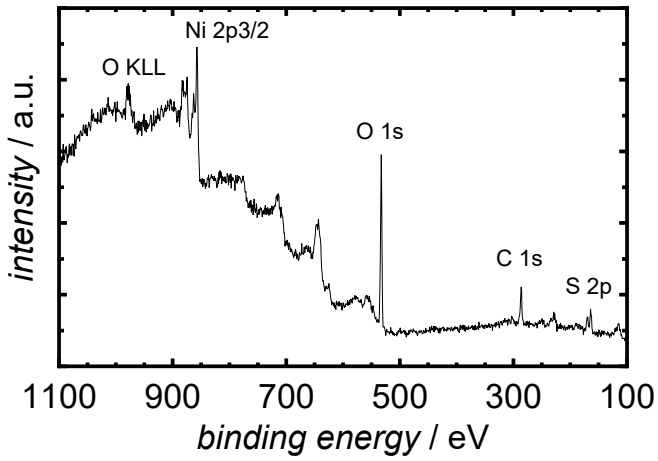

Fig. S18 XPS spectrum of NiS.

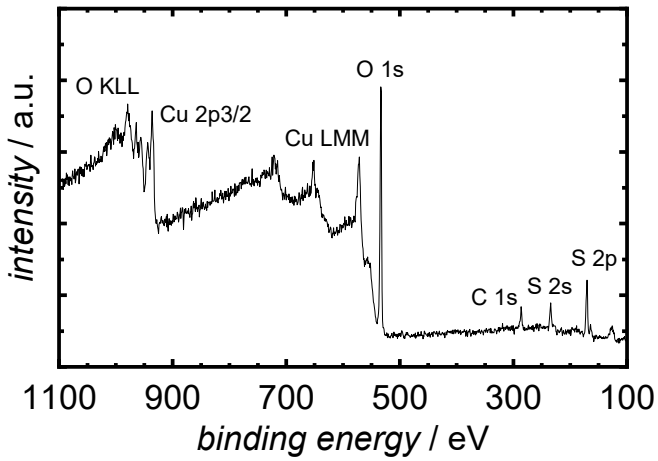

Fig. S19 XPS spectrum of CuS.

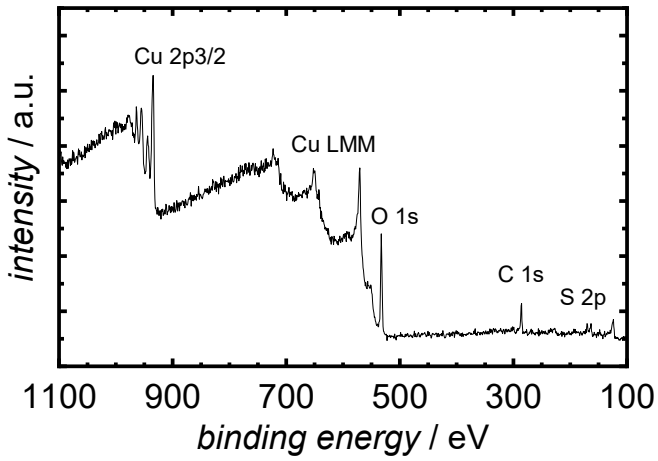

Fig. S20 XPS spectrum of Cu_2S.

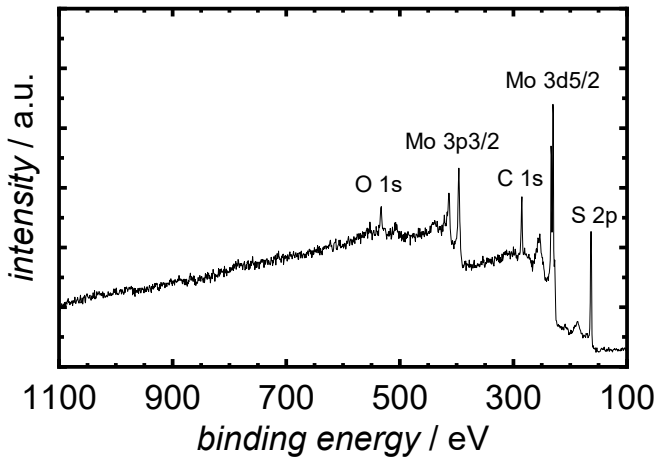

Fig. S21 XPS spectrum of MoS_2.

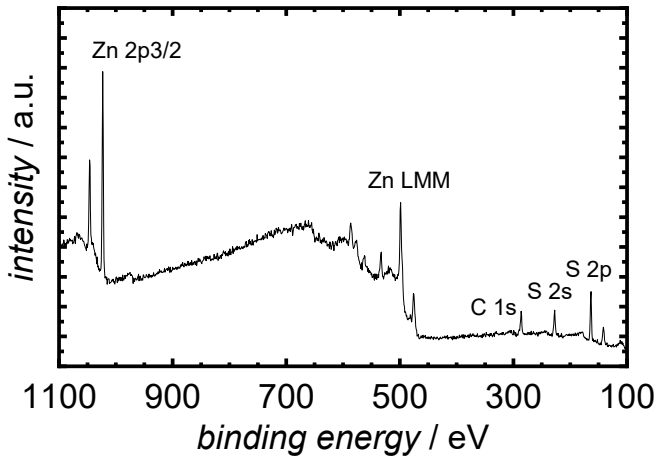

Fig. S22 XPS spectrum of ZnS.

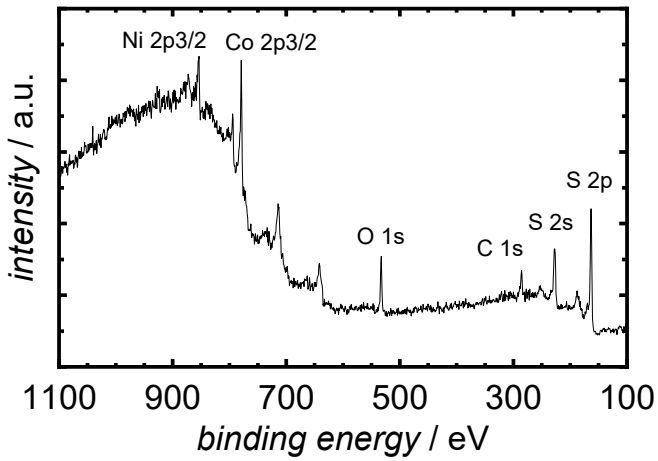

Fig. S23 XPS spectrum of $NiCo_2S_4$.

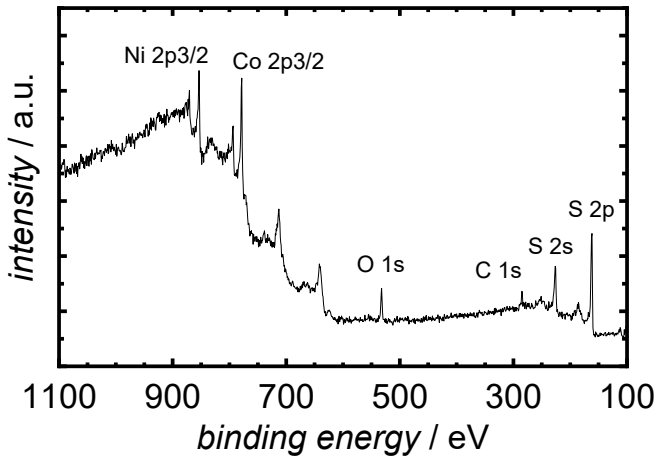

Fig. S24 XPS spectrum of $CoNi_2S_4$.

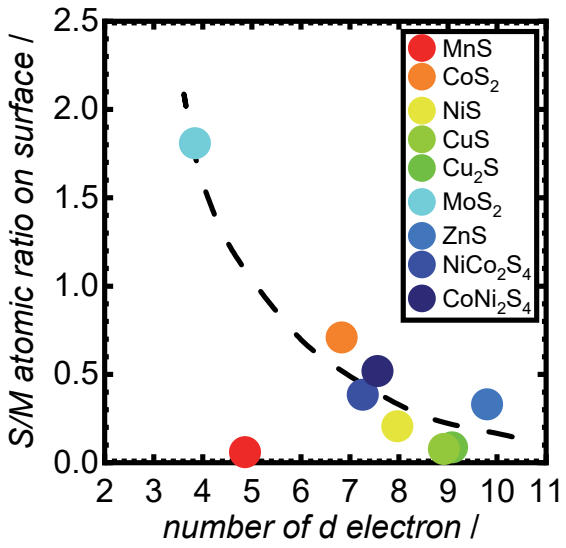

Fig. S25 S/M atomic ratios of each metal sulfides obtained by XPS measurements as a function of the number of *d* electrons in each metal component.

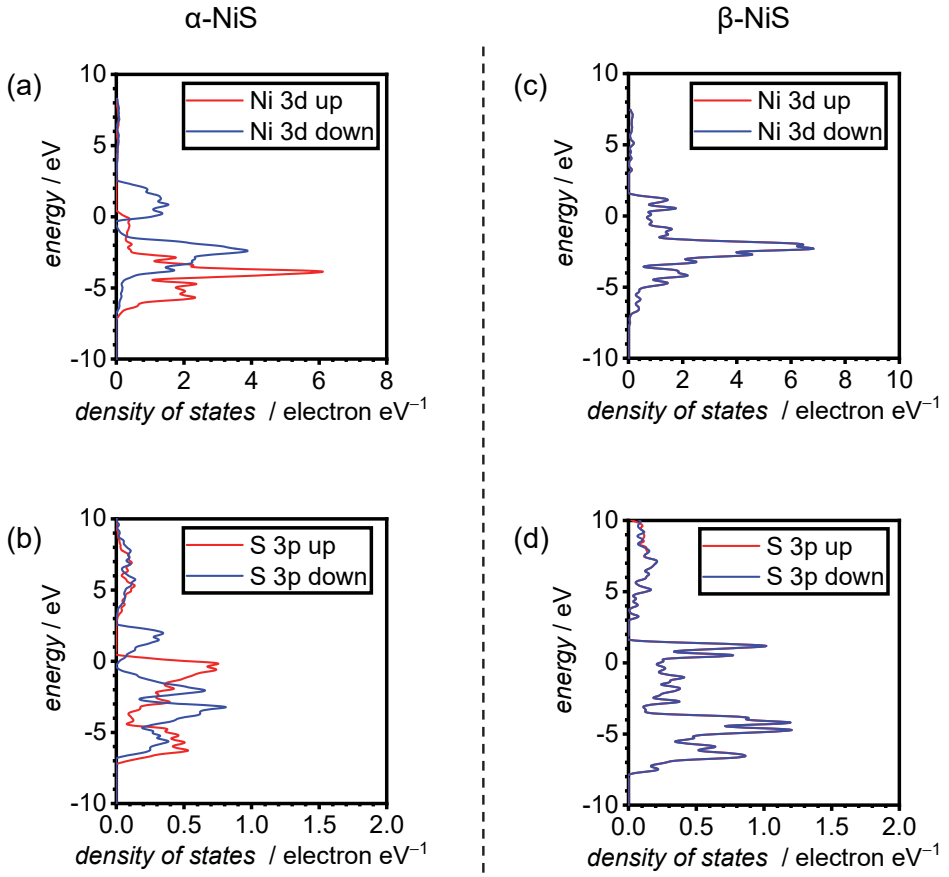

Fig. S26 DFT-calculated PDOS of the Ni *d* band and S *p* band for the metal sulfides. (a and b) *α*-NiS, (c and d) *β*-NiS.

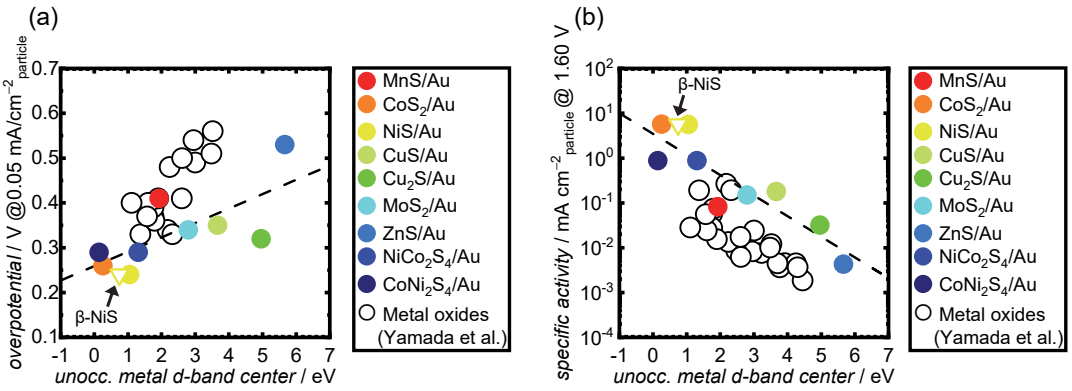

Fig. S27 The calculated data of β-NiS (yellow triangles), added to Fig. 7.

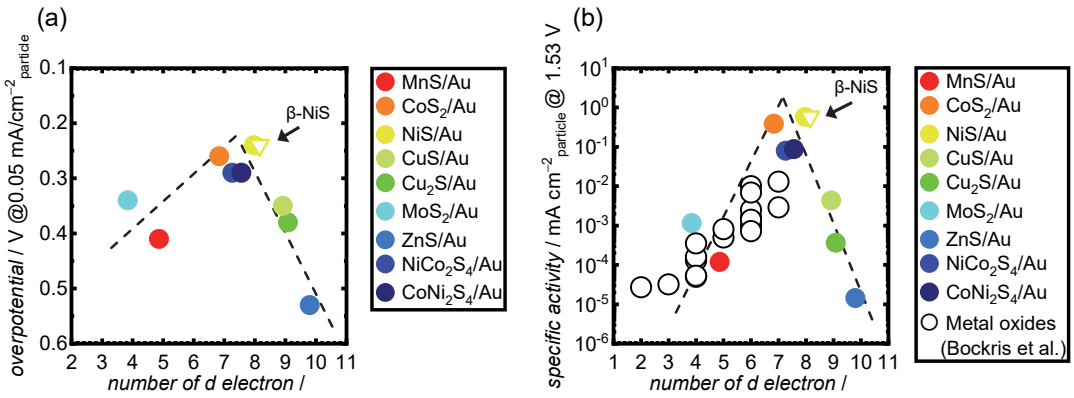

Fig. S28 The calculated data of β-NiS (yellow triangles), added to Fig. 8.

Table S1 Calculated unit cell sizes of the nine metal sulfides, the number of ***k***-points and *U*.

Catalyst	Lattice vector length[a] [Å]			***k***-point	*U*
MnS	5.221	5.221	5.221	8×8×8	N/A
CoS_2	5.528	5.528	5.528	7×7×7	3.3
NiS	3.440	3.440	5.348	12×12×8	3.6
β-NiS	5.640	5.640	5.640	8×8×8	3.6
CuS	3.794	3.794	16.341	11×11×3	4.0
Cu_2S	15.246	11.884	13.494	3×3×3	4.0
MoS_2	3.161	3.161	12.299	13×13×3	2.9
ZnS	3.793	3.793	43.811	11×11×1	N/A
$NiCo_2S_4$	9.382	9.382	9.382	4×4×4	Ni:3.6, Co:3.3
$CoNi_2S_4$	9.382	9.382	9.382	4×4×4	Ni:3.6, Co:3.3

[a]Initial structures obtained experimentally and collected as CIF formats from the JCPDS cards.

Table S2 Peaks observed in the Raman spectra of the metal sulfides in Fig. 2 compared with literature values.

Catalyst	Raman shift [cm^{-1}]		Ref.
	Expt. in this study	Reported	
MnS	320, 376, 660	319, 367, 657	1
CoS_2	288, 315, 392	292, 323, 393	2
NiS	239, 283, 333, 387, 473	140, 240, 300, 350, 380, 480[a]	3
CuS	263, 475	261, 472	4
Cu_2S	270, 471	265, 474	5
MoS_2	286, 383, 408, 452	284, 384, 408, 473	6
ZnS	153, 263, 347, 394, 417, 442, 613, 642	147, 176, 217, 262, 277, 348, 394, 422, 448, 522, 611, 638,	7
$NiCo_2S_4$	154, 249, 310, 356, 386	150, 239, 301, 342, 373	8
$CoNi_2S_4$	236, 308, 356, 388	230, 299, 351, 386	9

[a]Roughly estimated from the spectrum in the literature.

Table S3 Elemental compositions of $NiCo_2S_4$ and $CoNi_2S_4$.

Catalyst	Theoretical composition [wt%]	Measured composition[a] [wt%]
$NiCo_2S_4$	Ni 14.3, Co 28.6, S 57.1	Ni 17.5, Co 25.5, S 57.0
$CoNi_2S_4$	Ni 28.6, Co 14.3, S 57.1	Ni 26.2, Co 19.2, S 54.6

[a]Quantified by inductively coupled plasma–atomic emission spectroscopy.

Table S4 Unoccupied sulfur *p*-band centers in the metal sulfides determined from DFT calculations.

Catalyst	Unocc. *p*-band center of sulfur [eV]
MnS	1.32
CoS_2	0.267
NiS	1.31
β-NiS	0.866
CuS	4.23
Cu_2S	5.35
MoS_2	2.90
ZnS	5.47
$NiCo_2S_4$	1.19
$CoNi_2S_4$	0.153

Table S5 Elemental compositions of the metal sulfides.

Catalyst	Measured composition[a] [atom%]	Sulfur/Metal ratio [–]
MnS	Mn 94, S 6	0.059
CoS_2	Co 58, S 41	0.71
NiS	Ni 83, S 17	0.21
CuS	Cu 93, S 7	0.078
Cu_2S	Cu 92, S 8	0.087
MoS_2	Mo 36, S 64	0.33
ZnS	Zn 75, S 25	1.8
$NiCo_2S_4$	Ni 27, Co 44, S 27	0.38
$CoNi_2S_4$	Ni 27, Co 38, S 34	0.52

[a]Quantified by XPS.

References

1. M. Girish, T. Dhandayuthapani, R. Sivakumar, C. Sanjeeviraja and M. Kumaresavanji, *J. Mater. Sci.-Mater. Electron.*, 2017, **28**, 6741–6753.

2. D. Ma, B. Hu, W. D. Wu, X. Liu, J. T. Zai, C. Shu, T. T. Tsega, L. W. Chen, X. F. Qian and T. L. Liu, *Nat. Commun.*, 2019, **10**, 3367.

3. J. R. Xavier, S. P. Vinodhini and S. S. Chandraraj, *J. Clust. Sci.*, 2023, **34**, 1805–1817.

4. T. A. Estrada-Mendoza, T. F. Burgess, D. S. Edirisinghe, A. G. Gonzalez, J. N. Khalaf, J. Brentley Fravel, C. D. McMillen and G. Chumanov, *Chem. Method.*, 2022, **2**, e202100077.

5. R. A. Ismail, A. M. E. Al-Samarai and A. M. Muhammed, *J. Mater. Sci.-Mater. Electron.*, 2019, **30**, 11807–11818.

6. A. Taghizadeh, U. Leffers, T. G. Pedersen and K. S. Thygesen, *Nat. Commun.*, 2020, **11**, 3011.

7. A. Fairbrother, V. Izquierdo-Roca, X. Fontané, M. Ibáñez, A. Cabot, E. Saucedo and A. Pérez-Rodríguez, *CrystEngComm*, 2014, **16**, 4120–4125.

8. C. Xia, P. Li, A. N. Gandi, U. Schwingenschlögl and H. N. Alshareef, *Chem. Mater.*, 2015, **27**, 6482–6485.

9. C. E. Beckett-Brown, A. M. McDonald and W. Zhe, *Can. Mineral.*, 2018, **56**, 705–722.